Inorganic Chemistry

Article

pubs.acs.org/IC

Clusters $[M_a(GaCp^*)_b(CNR)_c]$ (M = Ni, Pd, Pt): Synthesis, Structure, and Ga/Zn Exchange Reactions

Mariusz Molon,[†] Katharina Dilchert,[†] Christian Gemel,[†] Rüdiger W. Seidel,[‡] Julian Schaumann,[§] and Roland A. Fischer*[,†]

[†]Inorganic Chemistry II-Organometallics & Materials, [‡]Department of Analytical Chemistry, and [§]Inorganic Chemistry III, Ruhr-Universität Bochum, D-44780 Bochum, Germany

Supporting Information

ABSTRACT: Reactions of homoleptic isonitrile ligated complexes or clusters of d^{10}-metals with the potent carbenoid donor ligand GaCp* are presented (Cp* = pentamethylcyclopentadienyl). Treatment of $[Ni_4(CNt\text{-}Bu)_7]$, $[\{M(CNR)_2\}_3]$ (M = Pd, Pt) and $[Pd(CNR)_2Me_2]$ (R = *t*-Bu, Ph) with suitable amounts of GaCp* lead to the formation of the heteroleptic, tri- and tetranuclear clusters $[Ni_4(CNt\text{-}Bu)_7(GaCp^*)_3]$ (**1**), $[\{M(CNt\text{-}Bu)\}_3(GaCp^*)_4]$ (M = Pd: **2a**, Pt: **2b**), and $[\{Pd(CNR)\}_4(GaCp^*)_4]$ (R = *t*-Bu: **3a**, Ph: **3b**). The reactions involve isonitrile substitution reactions, GaCp* addition reactions, and cluster formation reactions. The new compounds were investigated for their ability to undergo Ga/Zn exchange reactions when treated with $ZnMe_2$. The novel tetranuclear Zn-rich clusters $[Ni_4GaZn_7(Cp^*)_2Me_7(CNt\text{-}Bu)_6]$ (**4**) and $[\{Pd(CNR)\}_4(ZnCp^*)_4(ZnMe)_4]$ (R = *t*-Bu: **5a**, Ph: **5b**) were obtained and isolated. The electronic situation and geometrical arrangement of atoms of all compounds will be presented and discussed. All new compounds are characterized by solution ^1H, ^{13}C NMR and IR spectroscopy, elemental analysis (EA), liquid injection field desorption ionization mass spectrometry (LIFDI-MS) as well as single crystal X-ray crystallography.

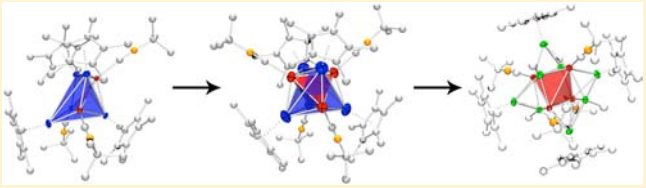

INTRODUCTION

GaCp* ligated transition metal complexes $[M(GaCp^*)_n]$ undergo a unique Ga/Zn and Cp*/Me exchange when treated with $ZnMe_2$ to form a new family of zinc-rich, highly coordinated molecules $[M(ZnR)_{2n}]$, ($n \geq 4$; M = Mo, Ru, Rh, Ni, Pd, Pt; R = Me, Et, Cp*).[1,2] A series of homoleptic compounds $[M(ZnR)_n]$ has been described, which all exhibit a regular 18 valence electron (VE) count of the central metal M, that is, the number of ZnR ligands ($2n$) can be predicted by the nature of the transition metal M, that is, its position in the Periodic Table ($2n = 18 - N$; N = group number). Computational studies on the density functional theory (DFT) level of theory suggest an electronic situation in this class of complexes with strong radial M-Zn bonding, that is, a bonding situation similar to classical Werner-type complexes. However substantial electronic density is also found in the ligand shell (Zn−Zn interactions), and the overall electronic situation can be described somewhere between a classic coordination compound and an intermetallic phase in the solid state. In fact this point of view has been positively probed by the synthesis of the intermetallic cluster $[\{(CO)_4Mo\}_4(Zn)_6(ZnCp^*)_4]$, which is formed in high yields in the reaction of $[(CO)_4Mo(GaCp^*)_2]$ and $ZnMe_2$.[3,4] In this compound four tetrahedrally arranged Mo atoms are connected by six naked Zn atoms, which are located on each Mo−Mo edge. Most interestingly, this exact Mo_4Zn_6 block is also found as a structural element in the Zn rich intermetallic Mo/Zn phase $MoZn_{20.44}$. One could speculate that the proper mix of electron donating Cp* and electron accepting carbonyl ligands in the reaction mixture is perfectly suitable for the electronic stabilization of a real "cut-out" of the Mo−Zn Hume−Rothery phase $MoZn_{20.44}$, which will exhibit polarized metal centers due to the electronegativity difference of Mo and Zn. Inspired by these results we were further interested in the synthesis of Zn-rich compounds $[M_a(ZnR)_bL_c]$ with a higher transition metal content ($a \geq 3$), aiming at extended molecular models of intermetallic phases of the M/Zn Hume−Rothery family. Although the presence of electron accepting ligands is obviously crucial for cluster formation, many other factors, such as the M:Ga ratio in the starting complexes, also determine the nature of the products, and in many cases the outcome remains unpredictable.[4−8] Yet, the availability of suitable electron poor complexes $[M_a(ECp^*)_bL_c]$ (L = CO or other electron withdrawing ligands) is rather limited (e.g., see publications from Grachova, E.; Scheer, M.; Jutzi, P., and our group).[9−13] In this contribution we wish to report on our results on the synthesis and characterization of novel compounds $[M_a(GaCp^*)_bL_c]$ (L = CN*t*-Bu; M = Ni, Pd, Pt), as well as the outcome of subsequent, selective Ga/Zn exchange by treatment with $ZnMe_2$. In particular we discuss the characterization, structural properties, and application of formal electron counting rules for the obtained clusters.

Received: August 31, 2013
Published: November 27, 2013

Table 1. Relationship between Precursor Compounds and the Isolated Products 1−3b

precursor	eq. GaCp*	product
$[Ni_4(CNt\text{-}Bu)_7]$	3	$[Ni_4(CNt\text{-}Bu)_7(GaCp^*)_3]$ (**1**)
$[\{Pd(CNt\text{-}Bu)_2\}_3]$	excess	$[\{Pd(CNt\text{-}Bu)(\mu_2\text{-}GaCp^*)\}_3(\mu_3\text{-}GaCp^*)]$ (**2a**)
$[\{Pt(CNt\text{-}Bu)_2\}_3]$	excess	$[\{Pt(CNt\text{-}Bu)(\mu_2\text{-}GaCp^*)\}_3(\mu_3\text{-}GaCp^*)]$ (**2b**)
$[\{Pd(CNt\text{-}Bu)_2\}_3]$	1	$[\{Pd(CNt\text{-}Bu)(\mu_2\text{-}GaCp^*)\}_4]$ (**3a**)
$[Pd(CNt\text{-}Bu)_2(Me)_2]$	2.3	$[\{Pd(CNt\text{-}Bu)(\mu_2\text{-}GaCp^*)\}_3(\mu_3\text{-}GaCp^*)]$ (**2b**)
$[Pd(CNPh)_2(Me)_2]$	2	$[\{Pd(CNPh)\}_4(\mu_4\text{-}GaCp^*)_2(\mu_2\text{-}GaCp^*)_2]$ (**3b**)

Scheme 1. Synthesis of 1−3b Starting from $[Ni_4(CNt\text{-}Bu)_7]$, $[\{M(CNt\text{-}Bu)_2\}_3]$ (M = Pd, Pt), or $[Pd(CNR)_2(Me)_2]$ (R = *t*-Bu, Ph)

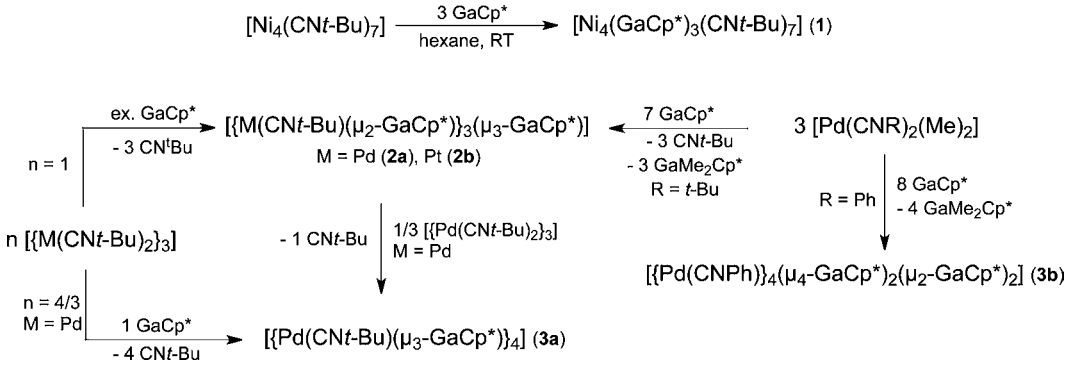

Scheme 2. Synthesis of 4, 5a, and 5b

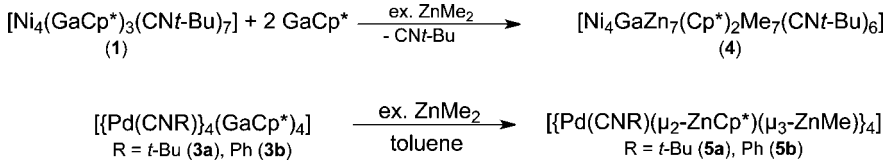

RESULTS AND DISCUSSION

Synthesis and Composition of M/Ga and M/Zn Mixed Complexes. Several homoleptic mono-, tri-, and tetranuclear d^{10} transition metal complexes with isonitrile ligands (Table 1) were reacted with GaCp* in various stoichiometric ratios to give mixed metal cluster compounds, stabilized by both, remaining isonitrile as well as GaCp* ligands.

In the case of $[Ni_4(CNt\text{-}Bu)_7]$, the nuclearity of the Ni_4 core is maintained without the loss of isonitriles, three GaCp* ligands are added and coordinate to the metal core of the reaction product. Reaction of GaCp* with trimeric complexes $[\{M(CNt\text{-}Bu)_2\}_3]$ (M = Pd, Pt), leads to formation of M_3 and Pd_4 clusters, depending on the molar ratios of reactants. Similarly, $[Pd(CNR)_2(Me)_2]$ forms tri- and tetrameric clusters through reduction of the palladium center by GaCp* (which itself is oxidized to $[Cp^*GaMe_2]$ via methyl-group transfer). However, the nuclearity of the resulting product in these cases is rather a consequence of the steric nature of the isonitrile ligand and not of the molar ratio of the reactants. Scheme 1 illustrates the details for all these cluster formation reactions.

In a second step, these mixed metal Ni/Ga and Pd/Ga clusters (Table 1, Scheme 1) were treated with $ZnMe_2$ to achieve a controlled Ga/Zn exchange. However, treatment of **2a**, **2b**, or **3c** with $ZnMe_2$ leads to rapid decomposition and precipitation of metal particles, while **1**, **3a**, or **3b** react with $ZnMe_2$ (in the presence of additional GaCp*, if needed) to yield the defined M/Zn(Ga) clusters $[Ni_4GaZn_7(Cp^*)_2Me_7(CNt\text{-}Bu)_6]$ (**4**) and $[\{Pd(CNR)(\mu_2\text{-}ZnCp^*)(\mu_3\text{-}ZnMe)\}_4]$ (R = t-Bu: **5a**, Ph: **5b**) (Scheme 2).

Spectroscopic Characterization. All new compounds were characterized by high-resolution ^1H and ^{13}C nuclear magnetic resonance (NMR) and by Fourier transform infrared spectroscopy using attenuated total reflection (FTIR-ATR). The molecular composition was determined by elemental analysis and mass spectrometry, using a liquid injection field desorption ionization method (LIFDI). These results are in good agreement with the molecular structures in the solid state as determined by single crystal X-ray diffraction (XRD) studies.

All structures feature C−N stretching vibrations in the characteristic range for terminal isonitrile ligands (see Table 2), except for the Ni_4 cluster **1**, which is in good agreement to the molecular structures in the sold state (vide infra). ^1H and ^{13}C NMR spectra of compounds **1**−**5b** reveal one single resonance for each ligand (indicated by the resonances for the Cp*, *t*-Bu groups) with the proper ligand ratio consistent with the

Table 2. Listing of the Isonitrile ν(CN) IR Vibrations of Compounds 1−5b

compound	ν(C≡N) [cm^{-1}]
1	2002, 2074 (sh), 1733, 1707
2a	2068, 2036 (sh)
2b	2080, 3037 (sh)
3a	2067, 2036
3b	2036, 1976 (sh)
4	2066 (sh), 2006
5a	2093, 2034 (sh)
5b	2045, 1968 (sh)

dx.doi.org/10.1021/ic4022189 | Inorg. Chem. 2013, 52, 14275−14283

molecular structure in the solid state, unless otherwise stated (see Experimental Section for details).

Molecular Structures in the Solid State. Important crystallographic data are summarized in the Supporting Information, Table S1, and the molecular structures deduced from the XRD and spectroscopic data are shown in Figures 1−6. Whereas **1**, **3a**, and **5** show a regular M_4 tetrahedron (M = Ni, Pd), **4** possess a butterfly structure, and **3b** is arranged in a square planar fashion. Both M_3 clusters **2a** and **2b** are arranged in a regular triangular way. Selected interatomic distances of transition metals in these clusters are presented in Table 3 and are found to be strongly distorted in the case of **1** or **4**, which range from 2.408(1) to 2.849(1) Å. These are longer as compared to the starting material $[Ni_4(CNt\text{-}Bu)_7]$ (2.338 Å), but are well comparable to several isoelectronic tetrahedral complexes like $[Ni_4(CO)_6L_4]$ with L = GaCp* (2.437−2.659 Å, a.v. 2.578 Å),[14] PMe_3,[15] $P(n\text{-}Bu)_3$,[15] and $P(C_2H_4CN)_3$.[16] In a similar way the interatomic M-M distances of the other compounds are significantly longer than found in the corresponding starting materials, but are well comparable to those of complexes like $[\{M(\mu_2\text{-}Sn(NR_2)_2)(CO)\}_3]$ (M = Pd: a.v. 2.81 Å, Pt: a.v. 2.76 Å; R = $SiMe_3$) with a trinuclear structure or almost linearly arranged $[Pd_3(GaCp^*)_4(\mu_2\text{-}GaCp^*)_4]$ (2.843(5) Å).[17,18] In comparison to interatomic distances in the bulk of Ni (2.492 Å), Pd (2.745 Å) and Pt (2.770 Å) the M-M distances are found to be longer in all cases for **1**−**5b**.[19,20]

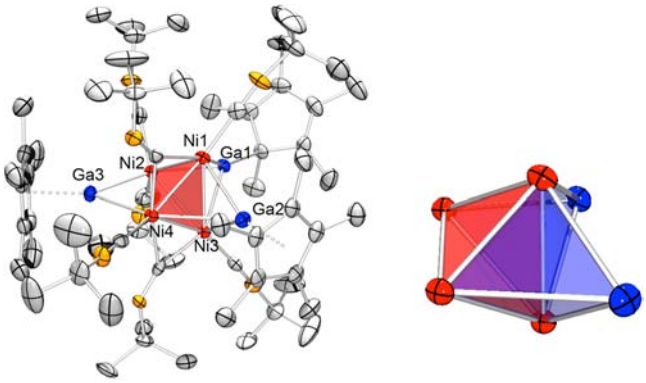

Figure 1. Povray plot of the molecular structure of **1** (left) and the core structure (right, each three Ni atoms and face-capping Ga atoms are interconnected to planes to guide the eye of the observer) in the solid state as determined by single crystal X-ray diffraction (thermal ellipsoids are shown at the 50% probability level, C and N atoms were displayed as isotropic spheres for clarity, hydrogen atoms were omitted). Selected bond length and distances (Å): Ni−Ni: 2.394(1)−2.887(1), Ga1−Ni: 2.327(1)−2.399(1), Ga2−Ni1: 2.354(1)−2.364(1), Ga3−Ni2: 2.323(1)−2.478(1), C≡N(5/6): a.v. 1.21, other C≡N: a.v. 1.17, Ga−Cp*: a.v. 2.05, Ni−C≡$N_{terminal}$: a.v. 1.81, Ni−C≡$N_{bridging}$: a.v. 1.93, Ni−C≡$N_{terminal}$: a.v. 173.2, Ni−C≡$N_{bridging}$: a.v. 140.4.

M-Ga as well as M-Zn distances of compounds **1**−**5b** are longer than those found in the homoleptic mononuclear compounds $[M(GaCp^*)_4]$ and $[M(ZnCp^*)_4(ZnMe)_4]$ (M = Ni, Pd, Pt).[14,21,22] This observation is in good agreement with the fact that the organo gallium and organo zinc ligands of **1**−**5b** are arranged in bridging bonding modes following the trend of distances M-(μ_2-GaCp*) < M-(μ_3-GaCp*) < M-(μ_4-GaCp*) (see Table 3). Compound **1** is an exception to this trend which is based on different hapticity mode of Cp* at Ga1. A similar trend M-(μ_2-ZnR) < M-(μ_3-ZnR) can be observed for organo zinc ligands found in compound **4**, **5a**, and **5b**. No unusually short Ga−Ga or Zn−Zn distances were observed, that is, no significant attractive interactions are found in the ligand shell of the clusters. In the following sections specific characteristics of each molecular structure will be discussed briefly.

$[Ni_4(GaCp^*)_3(CNt\text{-}Bu)_7]$ (1). The GaCp* ligands appear in a bridging or face capping bonding mode in the coordination sphere of **1** (see Figure 1). Three nickel atoms (Ni1, Ni3, and Ni4) are ligated by one, Ni2 by two *tert*-butylisonitrile ligands. Furthermore two edges of the Ni_4 tetrahedron (Ni4−Ni1 and Ni4−Ni3) are bridged by one *tert*-butylisonitrile ligand, each. As expected, the terminally coordinated isocyanides in **1** show shorter N−C distances (1.155−1.176 Å, a.v. 1.167 Å) than the bridging isocyanides (1.191−1.222, a.v. 1.212 Å). The C−N−CMe_3 angles of terminally bonded isonitriles are close to linear with values of average 173.2° while the corresponding bridged ones deviate significantly from linearity by about 22% (a.v. 140.4°).

The ^{1}H NMR spectrum of **1** shows a number of overlapping signals in the expected areas for GaCp* and isonitrile ligands, which is in good agreement with the highly asymmetric arrangement of the ligands and their different bonding modes. At 100 °C in toluene-d_8, all signals coalesce to one broad resonance for the GaCp* ligands (1.93 ppm) and one broad resonance for the *tert*-butylisonitrile ligands (both, bridged and terminal) (1.4 ppm) with an integral ratio of 45:63 corresponding to the ligand ratio GaCp*: *t*-BuNC of 3:7.

$[\{M(CNt\text{-}Bu)(\mu_2\text{-}GaCp^*)\}_3(\mu_3\text{-}GaCp^*)]$ (M = Pd: 2a, Pt: 2b). The transition metal atoms are arranged in an isosceles triangular composition with almost ideal values of 60°. This metal triangle is face capped by one GaCp* ligand and all three edges of the mentioned triangle are bridged by one GaCp* moiety each, leading to a distorted tetrahedral arrangement of the Ga atoms only (see Figure 2). There are two sets of Ga−Ga

Table 3. Selected Interatomic Distances Found in Compounds 1−5b (E = Ga/Zn)

	M-M	M-(μ_2-E)	M-(μ_3-E)
1	2.408(1)−2.839(1)	2.323(1)−2.478(1)	2.342(1)−2.399(1)[a]
2a	2.815(1)−2.849(1)	2.441(1)−2.477(1)	2.516(1)−2.529(1)
2b	2.788(1)−2.827(1)	2.437(1)−2.471(1)	2.525(1)−2.543(1)
3a	2.875(2)		2.535(1)
3b	2.645(1)−2.843(1)	2.433(1)−2.453(1)	2.557(1)−2.658(1)[b]
4	2.555(1)−2.823(1)	2.332(1)−2.529(1)	2.419 (1)−2.633(1)
5a	2.827(1)−3.312(1)	2.517(1)−2.548(1)	2.569(1)−2.611(1)
5b	2.820(1) and 3.201(1)	2.520(1) and 2.536(1)	2.588(1)−2.603(1)

[a]Ga(η^1-Cp*). [b]M-(μ_4-E).

dx.doi.org/10.1021/ic4022189 | Inorg. Chem. 2013, 52, 14275−14283

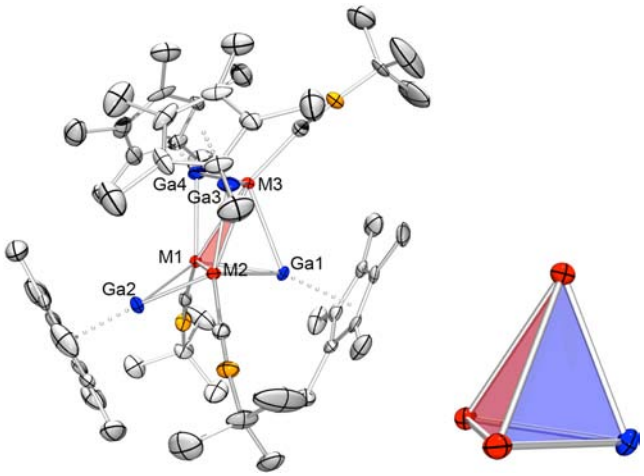

Figure 2. Povray plot of the molecular structure of **2a** and **2b** (left) and the core structure (right, each three Pd/Pt atoms and face-capping Ga atoms are interconnected to planes to guide the eye of the observer) in the solid state as determined by single crystal X-ray diffraction (thermal ellipsoids are shown at the 50% probability level, hydrogen atoms were omitted). Selected bond length and distances (Å), as well as angles (deg) are summarized in Table 4

vectors representing the compressed nature of the proposed tetrahedron: On the one hand there are three Ga−Ga vectors (a.v. 3.872 Å) of shorter length and on the other hand three others (a.v. 4.460 Å) with a significantly higher value. The longer Ga−Ga vectors are found exclusively at the opposite site of Ga1, which is based on steric reasons.

Table 4. Selected Bond Length and Distances (Å), As Well As Angles (deg) of 2a and 2b

	2a	2b
M1−M2	2.849(1)	2.827(1)
M1−M3	2.815(1)	2.788(1)
M2−M3	2.818(1)	2.789(1)
Ga1−M	2.516(1)−2.529(1)	2.525(1)−2.543(1)
Ga2−M	2.448(1), 2.450(1)	2.439(2), 2.440(1)
Ga3−M	2.446(1), 2.477(1)	2.439(2), 2.467(2)
Ga4−M	2.441(1), 2.477(1)	2.437(2), 2.471(2)
M−C	1.971(6)−1.976(6)	1.913(11)−1.949(11)
N≡C	1.154(7)−1.158(7)	1.121(16)−1.163(15)
Ga−$Cp^*_{centroid}$	(a.v.) 2.051	(a.v.) 2.050
M−M−M	59.56(1)−60.76(1)	59.52(2)−60.91(2)
N≡C−M	172.7(5)−173.8(5)	174.0(11)−174.4(11)
C≡N−C	174.9(6)−176.4(6)	172.6(13)−175.4(13)

[{Pd(CN*t*-Bu)(μ_3-GaCp*)}$_4$] (3a). Because of a reversible temperature dependent phase change of **3a** single crystal measurements were obtained at 230 K only, since lower measurement temperatures resulted in loss of crystal quality and worse diffraction properties. Because of the comparably high measurement temperature and the present symmetry operations, the Cp* ligands are highly disordered along the Ga−$Cp_{centroid}$ vector, as well as the *tert*-butyl groups of the isocyanide ligand; therefore the peripheral atoms are shown as isotropic spheres. The Pd_4 tetrahedron (Figure 3) is four times face-capped by μ^3-GaCp* ligands (Figure 3, right).

[{Pd(CNPh)}$_4$(μ_4-GaCp*)$_2$(μ_2-GaCp*)$_2$] (3b). The Pd atoms in **3b** are arranged in a rectangular way with two shorter and two longer Pd−Pd vectors of 2.648(1), 2.645(1) and 2.791(1), 2.843(1) Å (see Figure 4). The shorter edges are bridged by one μ^2-GaCp* unit each. In addition the Pd_4 rectangle is capped by two μ^4-GaCp* ligands, one from each side, so that a Pd_4Ga_2 octahedron is formed (Figure 4, right). The ^{1}H NMR resonances of **3b** reveal one single resonance for the GaCp* ligands at 2.17 ppm beside three multiplet signals from the phenylrings. The dynamic behavior could not be frozen even at −80 °C revealing a fast fluxional process.

[Ni$_4$GaZn$_7$(Cp*)$_2$Me$_7$(CN*t*-Bu)$_6$] (4). The molecular structure, as depicted in Figure 5, consists of a nickel atom core with a butterfly structure together with two or one isonitrile ligand attached to each Nickel atom. The ligand shell is completed with seven bridging and face capped EMe (E = Zn/Ga) moieties, as well as two ECp* ligands. The position of Ga and Zn atoms cannot be assigned unambiguously from single crystal XRD measurements because of equal electron density maps of both atoms. The overall structure is rather complicated and not easy to describe because of a rather unsymmetrical arrangement. Interesting features are the Ni_4 butterfly like core, which is imbedded within a shell of nine metal atoms E (Ga/Zn). Three special coordination modes of E need to be mentioned: E7 is μ^4-bridging the Ni4 butterfly structure, E6 and E5 are face bridging over a Ni_3 triangle, and E2 is the only terminal one. All other positions of E are Ni_2 edge bridging.

[{Pd(CNR)}$_4$(ZnCp*)$_4$(ZnMe)$_4$] (R = *t*-Bu: 5a, Ph: 5b). Four Pd−Pd contacts are bridged by four ZnCp* ligands whereas four triangular faces of the Pd_4 tetrahedron are capped by four ZnMe ligands (see Figure 6). The inner Pd_4 tetrahedron is expanded along two edges, which were not bridged by ZnR units exclusively, with significantly larger distances of 3.154(1) and 3.312(1) Å for **5a** and 3.201(1) Å for **5b** in comparison to the other M-M contacts of 2.83 Å in average and 2.820(1) Å (see Table 5 for details).

Electron Counts in Clusters [M$_a$(GaCp*)$_b$(CNR)$_c$]. Counting electrons in intermetallic clusters like those presented in this paper follow simple electron counting rules like for example the borane clusters (Wade rules) or transition metal carbonyl clusters ($14n$ + 2 for four-connect clusters and $15n$/$16n$ rules for three-connect clusters). However, including GaCp* as a part of such clusters poses the immediate problem of whether the gallium atom is considered as part of the metal core structure or rather takes the role of a simple $2e^-$ donor ligand. Both are possible. The answer to this question seems to be obvious in all compounds discussed in the paper: All face bridging GaCp* groups (i.e., gallium atoms, which are directly connected to three or more metal atoms) are considered as part of the metal core structure, whereas terminal GaCp* groups are counted as simple $2e^-$ donor ligands instead. Edge-bridging gallium atoms are most often best considered as two electron donor ligands, but exceptions are possible (e.g., the cluster [Pd_3(GaCp*)$_8$] discussed below) [{Pd(CNPh)}$_4$(μ_4-GaCp*)$_2$(μ_2-GaCp*)$_2$] (**3b**), for example represents a regular octahedral Pd_4Ga_2 core (*closo* structure). Its structure can be predicted by the $14n$ + 2 rule (n = 4) for Pd and $4n$ + 2 rule (n = 2) for Ga leading to a total number of cluster VEs of 58 + 10 = 68, which is exactly the number of VEs in **3b** (see Table 6). Another representative example is the homoleptic cluster [Pd_3(μ_2-GaCp*)$_4$(GaCp*)$_4$][18] consisting of two vertex-bridging square Pd_2Ga_2 units (i.e., four GaCp* ligands in total are considered as part of the metal core structure). Each Pd_2Ga_2 unit coordinated by two additional GaCp* ligands (i.e., four GaCp* in total are considered as 2e- donor ligands only). Following the counting rules outlined above, two *arachno*-

dx.doi.org/10.1021/ic4022189 | *Inorg. Chem.* 2013, 52, 14275−14283

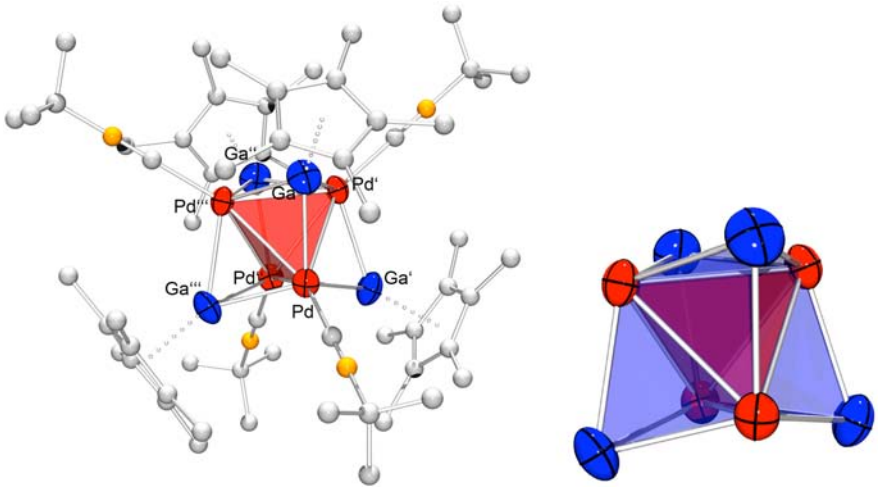

Figure 3. Povray plot of the molecular structure of **3a** (left) and the core structure (right, each three Pd atoms and face-capping Ga atoms are interconnected to planes to guide the eye of the observer) in the solid state as determined by single crystal X-ray diffraction (thermal ellipsoids are shown at the 50% probability level, C and N atoms were displayed as isotropic spheres, hydrogen atoms were omitted). Selected bond length and distances (Å), as well as angles (deg): Pd−Ga: 2.535(1), Pd−Pd: 2.875(2), Ga−Ga: 4.087, Pd−C: 1.97(2), C≡N: 1.08(2), Ga−Cp*$_{centroid}$: 2.083, Pd−Pd−Pd: 60.00, Ga−Pd−Ga: 107.44(3), Pd−Ga−Pd: 69.09, N≡C−Pd: 180(2), C≡N−C: 180(2).

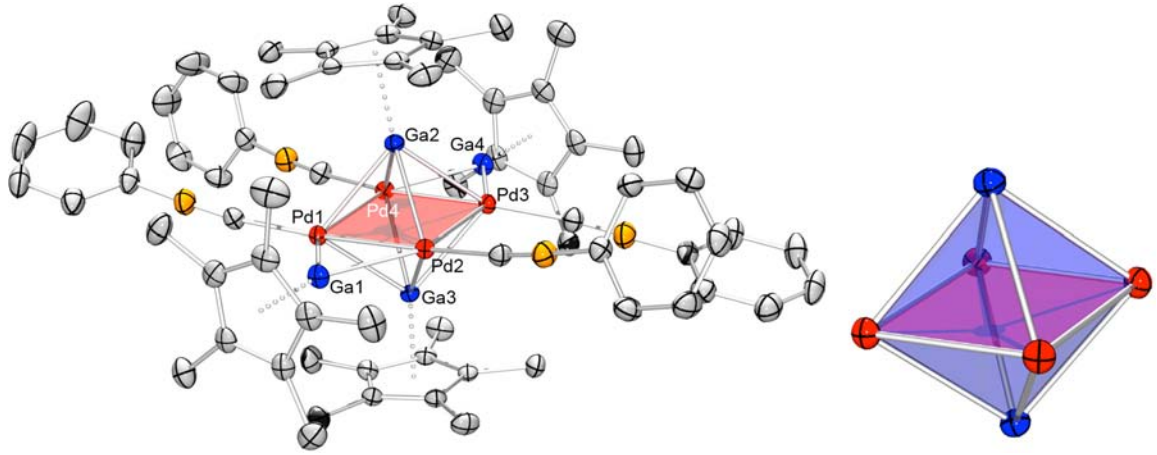

Figure 4. Povray plot of the molecular structure of **3b** (left) and the core structure (right, each three Ni atoms and face-capping Ga atoms are interconnected to planes to guide the eye of the observer) in the solid state as determined by single crystal X-ray diffraction (thermal ellipsoids are shown at the 50% probability level, hydrogen atoms were omitted). Selected bond length and distances (Å), as well as angles (deg): Pd1−Pd2: 2.648(1), Pd3−Pd4: 2.645(1), Pd2−Pd3: 2.791(1), Pd1−Pd4: 2.843(1), Pd−Ga1: 2.452(1) and 2.435(1), Pd−Ga2: 2.557(1)−2.622(1) (a.v. 2.59), Pd−Ga3: 2.574(1)−2.658(1) (a.v. 2.60), Pd−Ga4: 2.433(1) and 2.453(1), Pd−C: 1.962(3)−1.978(3) (a.v. 1.97), N≡C: 1.156(4)−1.165(1) (a.v. 1.16), Ga$_{apical}$−Cp*$_{centroid}$: 2.073 and 2.080, Ga$_{bridging}$−Cp*$_{centroid}$: 2.011 and 2.018.

Pd_2Ga_2 parts, which are connected via one Pd atom should show a cluster valence electron (CVE) count of 70, which exactly matches the CVE in $[Pd_3(\mu_2\text{-}GaCp^*)_4(GaCp^*)_4]$. Table 6 summarizes the CVE counts of all GaCp* containing clusters presented in this paper. Interestingly, the zinc-rich cluster compounds **4**, **5a**, and **5b** do not follow analogous counting rules. It should be noted, that the electron count of ZnCp* moieties is less by one electron as compared to the respective GaCp* species and the same is true for $ZnCH_3$ vs $GaCH_3$ and in case of face bridging $ZnCH_3$ moiety the electron count would be 3 rather than 8 for a GaCp* ligand counted as a part of the cluster core. Thus, the Ga/Zn exchange reaction with the rule of two ZnR species being incorporated for one GaR also involving CH_3/Cp* exchange for R drastically changes the electron count situation. The steric demand of ZnR is similar to GaR (R = CH_3, Cp*), which means that the zinc-rich compounds **4**, **5a−b** are more crowded than the gallium-rich clusters **1**, **2a−b**, **3a−b**. These circumstances need to be taken into account and may be the origin of deviation from simple CVE counting rules and respective structure prediction/rationalization.

CONCLUSION

We investigated the reactivity of ECp* (E = Al, Ga) ligands toward multinuclear d^{10}-transition metal complexes stabilized by isonitrile ligands. In this course five tri- and tetranuclear cluster compounds $[Ni_4(CNt\text{-}Bu)_7(GaCp^*)_3]$ (**1**), $[\{M(CNt\text{-}Bu)\}_3(GaCp^*)_4]$ (M = Pd: **2a**, Pt: **2b**) and $[\{Pd(CNR)\}_4(GaCp^*)_4]$ (R = *t*-Bu: **3a**, Ph: **3b**) could be obtained. Besides, $[Pd(CNR)_2Me_2]$ (R = *t*-Bu, Ph) can also be used as starting material for the formation of **2a** or **3b**. Here the number of Pd atoms in the final product is selectively influenced by the isonitrile ligand used. Whereas CN*t*-Bu leads to a trinuclear compound, CNPh prefers to stabilize the

dx.doi.org/10.1021/ic4022189 | *Inorg. Chem.* 2013, 52, 14275−14283

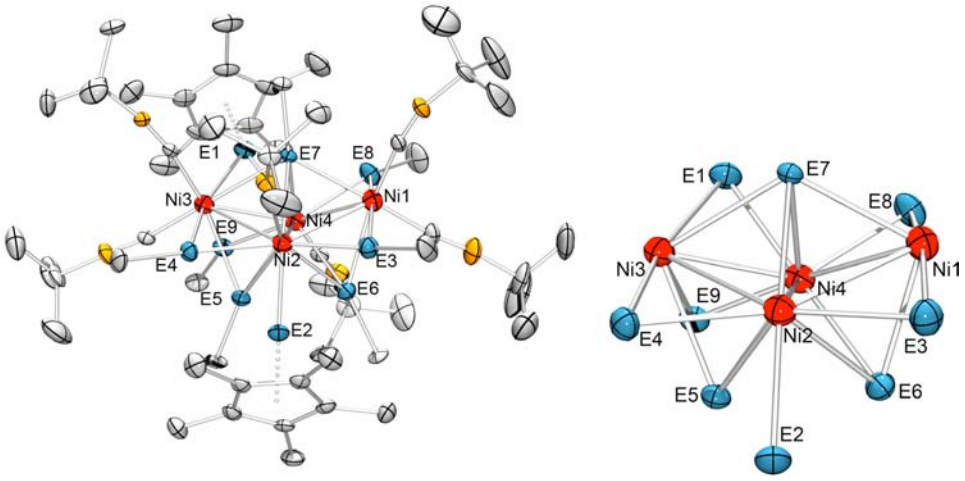

Figure 5. Povray plot of the molecular structure of **4** (left) and the core structure (right) in the solid state as determined by single crystal X-ray diffraction (thermal ellipsoids are shown at the 50% probability level, hydrogen atoms were omitted). Selected bond length and distances (Å), as well as angles (deg): Ni1−Ni2: 2.708(1), Ni1−Ni4: 2.637(1), Ni2−Ni3: 2.823(1), Ni2−Ni4: 2.740(1), Ni3−Ni4: 2.555(1), Ni−E1: 2.529(1) and 2.454(1), Ni2−E2: 2.355(1), Ni1−E: 2.405(1)−2.445(1) (a.v. 2.42), Ni2−E: 2.372(1)−2.490(1) (a.v. 2.43), Ni3−E: 2.508(1)−2.592(1) (a.v. 2.55), Ni4−E: 2.332(1)−2.633(1) (a.v. 2.47), E−E: 2.680(1)−3.135(1) (a.v. 2.90), Ni−C: 1.792(3)−1.848(3) (a.v. 1.82), N≡C: 1.152(4)−1.159(4) (a.v. 1.16), E1−$Cp^*_{centroid}$: 1.972, E2−$Cp^*_{centroid}$: 1.993, N≡C−Ni: 170.1(2)−177.4(3) (a.v. 172), C≡N−C: 161.5(3)−176.3(3) (a.v. 169).

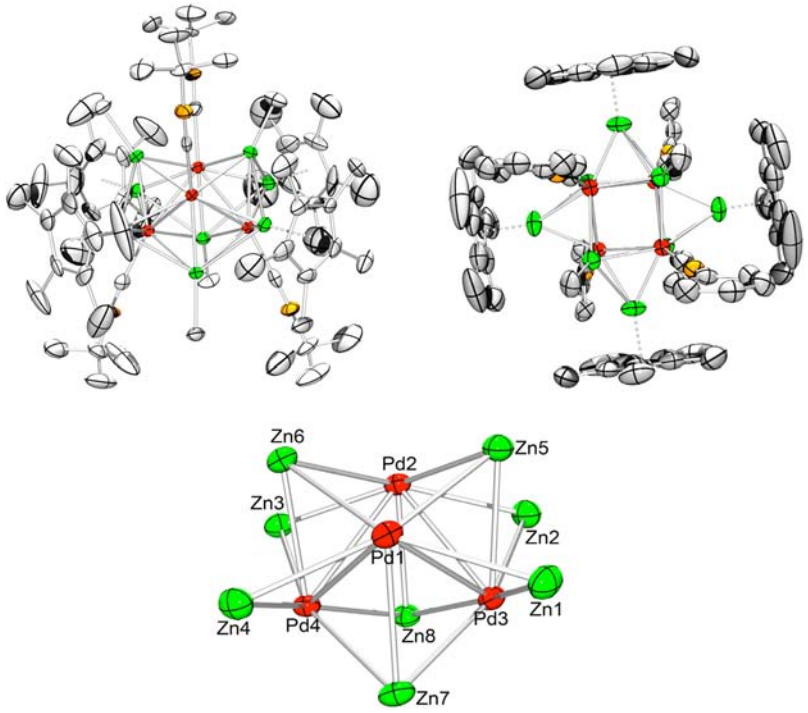

Figure 6. Povray plots of the molecular structures of **5a** (top left) and **5b** (top right) from different perspectives and the core structure (bottom) in the solid state as determined by single crystal X-ray diffraction (thermal ellipsoids are shown at the 50% probability level, hydrogen atoms were omitted). Selected bond length and angles are summarized in Table 5 of both compounds.

square planar arrangement of Pd atoms, whereas **3a** features a tetrahedral geometry. Furthermore, **2a** can be transferred to **3a** by treatment with 1 equiv of "[Pd(CN*t*-Bu)$_2$]", which is not possible with "[Pt(CN*t*-Bu)$_2$]"; accordingly the tetranuclear compound of Pt similar to **3a** was not observed at all, although cluster formation and building block synthesis of Pt was well examined.[21] Similar reactions with the more Lewis acidic AlCp* analogue failed because of selective C−N single bond cleavage of CN*t*-Bu irrespective if coordinated to a transition metal or as a free ligand (see Supporting Information). Furthermore $[Ni_4GaZn_7(Cp^*)_2Me_7(CNt\text{-}Bu)_6]$ (**4**) and $[\{Pd(CNR)\}_4(ZnCp^*)_4(ZnMe)_4]$ (R = *t*-Bu: **5a**, Ph: **5b**) could be obtained from Ga/Zn exchange reactions of **1**, **3a**, and **3b** with $ZnMe_2$. The cluster core-structures of the M/Ga/CNR mixed compounds can be easily derived by simple electron counting rules derived from transition metal carbonyl clusters. It was nicely shown that face capped (μ_3 and μ_4) GaCp* ligands are considered as part of the cluster core structure (vertex), whereas terminal, or edge bridged GaCp* ligands represent traditional two electron donor ligands. Remarkably,

dx.doi.org/10.1021/ic4022189 | *Inorg. Chem.* 2013, 52, 14275−14283

Table 5. Selected Bond Length and Distances (Å), As Well As Angles (deg) of 5a and 5b

	5a	5b
Pd1−Pd2	3.154(1)	3.201(1)
Pd3−Pd4	3.312(1)	3.201(1)[a]
all other Pd−Pd	2.827(1)−2.830(1) (a.v. 2.83)	2.820(1)
Pd−Zn(bridging)	2.517(1)−2.548(1) (a.v. 2.53)	2.520(1) and 2.536(1)
Pd−Zn(face-capped)	2.569(1)−2.611(1) (a.v. 2.59)	2.588(1)−2.603(1) (a.v. 2.60)
M-C	1.976(11)−2.016(10) (a.v. 2.00)	1.993(6)
N≡C	1.131(11)−1.185(12) (a.v. 1.16)	1.153(7)
Zn−$Cp^a_{centroid}$	1.962−1.977 (a.v. 1.97)	1.952
Pd1−Pd3−Pd2, Pd1−Pd4−Pd2	71.68(3) and 71.69(2)	69.15(1)
Pd4−Pd1−Pd3, Pd4−Pd2−Pd3	67.76(2) and 67.78(2)	69.15(1)[a]
other M−M−M	56.09(2)−56.15(2) (a.v. 56.1)	55.42(1) and 69.15(1)[a]
N≡C−M	175.9(9) −177.9(9) (a.v. 177)	174.6(5)
C≡N−C	175.1(11)−178.3(11) (a.v. 177)	174.9(6)

[a]Symmetry equivalent values.

Table 6. Electron Count of Compounds 1−3b

		M	GaCp*[a]	GaCp*[b]	CNR	CVE
$[Ni_4(CNt\text{-}Bu)_7(GaCp^*)_3]$ (**1**)	Ni_4Ga_2 2-fold capped tetrahedron	40	16	2	14	72
$[\{M(CNt\text{-}Bu)(\mu_2\text{-}GaCp^*)\}_3(\mu_3\text{-}GaCp^*)]$ (**2a**/**2b**)	M_3Ga tetrahedron	30	8	6	6	50
$[\{Pd(CNt\text{-}Bu)(\mu_2\text{-}GaCp^*)\}_4]$ (**3a**)	Pd_4Ga_4 4-fold capped tetrahedron	40	32		8	80
$[\{Pd(CNPh)\}_4(\mu_4\text{-}GaCp^*)_2(\mu_2\text{-}GaCp^*)_2]$ (**3b**)	Pd_4Ga_2 octahedron	40	16	4	8	68
$[Pd_2(\mu_2\text{-}GaCp^*)_3(GaCp^*)_2]$[18]	Pd_2 linear unit	20		10		30
$[Pd_3(\mu_2\text{-}GaCp^*)_4(GaCp^*)_4]$[18]	Pd_3Ga_4 vertex fused squares	30	32	8		70

[a]As part of the cluster compound. [b]As a two e^- ligand

the zinc-rich cluster compounds **4**, **5a**, and **5b** do not follow analogous counting rules. Furthermore, the metal core structures discussed in this work do certainly not match directly with M/Zn/Ga intermetallic solid-state structures of Hume−Rothery type, but certain structure motifs like tetrahedral arrangements, face capped, or bridging motives and Zn/Ga exchange on certain positions are well-known from these solid-state materials. For example, an 8-fold capped and bridged tetrahedral structure, similar to **5a**, was found for example in the solid state structure of Pd_3Zn_{10}, but with inverted atom positions, here the central tetrahedron is built by a Zn_4 core structure with Pd atoms in the outer sphere.[23] Although we are still far from being able to predict the outcome of Ga/Zn exchange reactions (as found for **4**), we showed, within the scope of this work, that the nuclearity can be increased, if stabilizing agents of suitable σ/π-donor−acceptor properties and moderate steric demand, such as isonitrile ligands, are used as coligands at the transition metal centers. These obviously need some electron-withdrawing ligands to stabilize cluster species with a higher transition metal content. This might be a reason for the rapid decomposition and metal precipitation after treatment with $ZnMe_2$ of quite a number of all-GaCp* ligated transition metal complexes $[M_n(GaCp^*)_m]$ ($n \geq 2$), since $[Pd_2Zn_6Ga_2(Cp^*)_5Me_3]$[24] is the only compound of this type that could be isolated, yet. Further investigations on other electron poor transition metals coligated by CO and isonitrile ligands are currently under exploration, having the cluster compounds $[\{(CO)_4Mo\}_4(Zn)_6(ZnCp^*)_4]$ and $[Cp^*_2Rh][(Cp^*Rh)_6(Zn_6)(ZnCl)_{12}(\mu^6\text{-}Cl)]$ at the back of our minds.

EXPERIMENTAL SECTION

General Remarks. All manipulations were carried out in an atmosphere of purified argon using standard Schlenk and glovebox techniques. Hexane and toluene were dried using a MBraun Solvent Purification System. The final H_2O content in all solvents was checked by Karl Fischer titration and did not exceed 5 ppm. $[GaCp^*]$,[25] $[AlCp^*]$,[26,27] $[Ni_4(CNt\text{-}Bu)_7]$,[28,29] $[\{Pd(CNt\text{-}Bu)_2\}_3]$,[28,30] $[Pd(tmeda)(Me)_2]$,[31] $[\{Pt(CNt\text{-}Bu)_2\}_3]$,[32] and $[Pt(COD)_2]$[33,34] were prepared according to known methods from the literature. Elemental analyses were performed by the micro analytical laboratory at the Ruhr-University Bochum. NMR spectra were recorded on a Bruker Avance DPX-250 spectrometer (^1H, 250.1 MHz; ^{13}C, 62.9 MHz) in either C_6D_6 or C_7H_8 at room temperature (RT). Chemical shifts are given relative to TMS and were referenced to the solvent resonances as internal standards. The chemical shifts are described in parts per million (ppm), downfield shifted from TMS, and are consecutively reported as position (δH and δC), relative integral, multiplicity (s = singlet, m = multiplet), coupling constant (J in hertz (Hz)) and assignment.

Crystallography. The X-ray diffraction intensities from the crystals of the compounds **1**, **2a**, **3a**, **4a**, and **5a** were collected on an Oxford Xcalibur2 diffractometer with MoK_α radiation (λ = 0.71073 Å) and a Sapphire2 CCD; compounds **2b**, **3b**, and **5b** were measured on an Agilent SuperNova, Single source at offset diffractometer with CuK_α radiation (λ = 1.54184 Å) and an Atlas detector. The molecular structures were solved by direct methods using SHELXS-97 and refined against F^2 on all data by full-matrix least-squares with SHELXL-97.[35,36] The crystals were picked up with a glass fiber coated with a perfluoropolyether and immediately mounted in a cooled nitrogen stream of the diffractometer. Severely disordered cocrystallized solvent molecules were found in compounds **1**, **4**, and **5a**, which could not be modeled properly, and their contributions were removed from the diffraction data with PLATON/SQUEEZE.[37,38] CCDC 958127 (**1**), 958128 (**2a**), 958129 (**2b**), 958130 (**3a**), 958131 (**3b**), 958132 (**4**), 958133 (**5a**), 958134 (**5b**), and 958135 (**6**) contain the supplementary crystallographic data for this paper. These data can be obtained free of charge from the Cambridge Crystallographic Data Centre via www.ccdc.ac.uk/data_request/cif.

$[Ni_4(GaCp^*)_3(CNt\text{-}Bu)_7]$ (1). A reddish suspension of $[Ni_4(CNt\text{-}Bu)_7]$ (200 mg, 0.245 mmol) in hexane (5 mL) was treated at RT with an excess of GaCp* (6 equiv, 301 mg, 1.469 mmol). Within a few

dx.doi.org/10.1021/ic4022189 | Inorg. Chem. 2013, 52, 14275−14283

minutes the suspension turned to a dark red solution, which was stirred for additional 2 h at RT. After filtering small amounts of insoluble residues the solution was evaporated in vacuo to dryness and afterward washed with a small portion of cold hexane. Single crystals could be obtained out of a saturated solution in toluene when stored at −30 °C for several days. Yield: 294 mg (84%) of an orange powder. ^{1}H NMR (250.1 MHz, C_6D_6, 24 °C): δ = 2.39, 2.33, 2.12, 2.10, 2.00, 1.97, 1.94, 1.42, 1.39, 1.38, 1.37, 1.35, 1.33, 1.10, 1.03 ppm. $^{13}C\{^1H\}$ NMR (62.9 MHz, C_6D_6, 24 °C): δ = 113.2, 55.5, 31.7, 31.5, 31.4, 31.4, 31.2, 31.0, 31.0, 30.8, 30.7, 11.1, 10.6, 10.1 ppm. IR (ATR): 2002 (vs, C≡N), 1733 (s, C═N), 1707 (s, C═N), 1189 (s, C−N) cm^{-1}. No signals in LIFDI-MS (toluene). Elemental Anal. Calc. for $C_{65}H_{108}Ga_3N_7Ni_4$: C: 54.7; H: 7.6, N: 6.8; found: C: 54.1; H: 7.4; N: 6.9%.

[{Pd(CN*t*-Bu)(μ_2-GaCp*)}$_3$(μ_3-GaCp*)] (2a). *Method 1.* [Pd(tmeda)(Me)$_2$] (200 mg, 0.794 mmol) was suspended in hexane (5 mL), and CN*t*-Bu (2.2 equiv, 145 mg, 1.746 mmol) was added via syringe whereupon the suspension turned to a clear solution within a few minutes of stirring at RT. All volatile materials were removed in vacuo and redissolved in hexane (5 mL) and cooled to −80 °C whereupon the solution turned into a colorless suspension at that temperature. GaCp* (3 equiv, 488 mg, 2.381 mmol) was added, and the suspension was allowed to warm to RT within about 10 min; the suspension turned first into a orange solution, and after 5 min an orange precipitate was formed. To obtain full precipitation the amount of solvent was reduced to about 2 mL in vacuo and cooled to −78 °C. The supernatant was filtered off, and the residue was dried in vacuo overnight yielding 301 mg (96%) of an orange-red colored powder.

Method 2. [{Pd(CN*t*-Bu)$_2$}$_3$] (200 mg, 0.123 mmol) dissolved in toluene (5 mL) was treated with an excess of GaCp* (3 equiv, 452 mg, 2.206 mmol) whereupon the red solution turned deep red and a green precipitate formed within a few minutes. After 5 h of stirring at 100 °C no precipitate formed, when the reaction mixture was cooled down to RT. All volatile materials were evaporated in vacuo, and the resulting slurry was precipitated with hexane, which was cold filtered off. After drying the residue an orange-red powder can be obtained. Yield 138 mg (41%). ^{1}H NMR (250.1 MHz, C_6D_6, 24 °C): δ = 2.16 (60H, C_5**Me**$_5$), 1.30 (27H, CN*t*-**Bu**) ppm. $^{13}C\{^1H\}$ NMR (62.9 MHz, C_6D_6, 24 °C): δ = 167.3, 112.8, 55.4, 30.4, 10.6 ppm. IR (ATR): 2080 (vs, C≡N), 2049 (shoulder), 1198 (s, C−N) cm^{-1}. No signals in LIFDI-MS (toluene). Elemental Anal. Calc. for $C_{55}H_{87}Ga_4N_3Pd_3$: C: 47.6; H: 6.3; N: 3.0; found: C: 47.2; H: 6.2; N: 3.1%.

[{Pt(CN*t*-Bu)(μ_2-GaCp*)}$_3$(μ_3-GaCp*)] (2b). According to the synthesis of **2b** but [{Pt(CN*t*-Bu)$_2$}$_3$] (85 mg, 0.078 mmol) was used as the starting material. No precipitation was observed during the reaction. **3** was obtained in a yield of 80% (103 mg) after stirring at RT for 1 h and similar workup as in **2b**. ^{1}H NMR (250.1 MHz, C_6D_6, 24 °C): δ = 2.09 (60H, C_5**Me**$_5$), 1.43 (27H, CN*t*-**Bu**) ppm. $^{13}C\{^1H\}$ NMR (62.9 MHz, C_6D_6, 24 °C): δ = 167.7, 113.2, 55.9, 30.8, 11.1. ppm. IR (ATR): 2080 (vs, C≡N), 2037 (shoulder), 1192 (vs, C−N) cm^{-1}. LIFDI-MS (toluene): [M$^+$]: 1656.4, [M-Cp*$^+$]: 1517.2, [M-GaCp*$^+$]: 1448.2, [M-Ga$_2$Cp*$^+$]: 1312.2 *m*/*z*. Elemental Anal. Calc. for $C_{55}H_{87}Ga_4N_3Pt_3$: C, 40.0; H, 5.3; N: 2.5; found: C: 39.5; H: 4.9; N: 2.1%.

[{Pd(CN*t*-Bu)(μ_3-GaCp*)}$_4$] (3a). *Method 1.* Reddish [{Pd(CN*t*-Bu)$_2$}$_3$] (100 mg, 0.123 mmol) was solved in hexane (5 mL), and GaCp* (75 mg, 0.368 mmol) is added via syringe whereupon a green microcrystalline precipitate is formed immediately. After 10 min of stirring at RT all volatile materials were evaporated in vacuo. The green precipitate reversibly changed color to orange during the drying process and turned green when treated with small amounts of hexane or other non coordinating solvents. The residue was washed with a small amount of cold hexane and dried in vacuo yielding 117 mg (81%) of orange colored powder.

Method 2. [{Pd(CN*t*-Bu)(μ_2-GaCp*)}$_3$(μ_3-GaCp*)] (**2a**, see above). (100 mg, 0.072 mmol) was treated with a third equivalent of [{Pd(CN*t*-Bu)$_2$}$_3$] (20 mg, 0.024 mmol) whereupon a fast green precipitate formed in quantitative yields. Workup was done as described in method 1 above. ^{1}H NMR (250.1 MHz, C_6D_6, 24 °C): δ = 2.30 (60H, C_5**Me**$_5$), 1.31 (36H, CN*t*-**Bu**) ppm. $^{13}C\{^1H\}$ NMR (62.9 MHz, C_6D_6, 24 °C): δ = 112.3, 38.2, 30.4, 11.2 ppm. IR (ATR): 2067 (vs, C≡N), 2036 (vs, C≡N), 1196 (vs, C−N) cm^{-1}. LIFDI-MS (toluene): [M$^+$]: 1578.5, [M-Cp*$^+$]: 1444.6, [M-GaCp*$^+$]: 1372.5 *m*/*z*. Elemental Anal. Calc. for $C_{60}H_{96}Ga_4N_4Pd_4$: C: 45.8; H: 6.2; N: 3.6; found: C: 45.3; H: 5.8; N: 3.1%.

[{Pd(CNPh)(μ_3-GaCp*)}$_4$] (3b). [Pd(tmeda)Me$_2$] (200 mg, 0.794 mmol) was suspended in hexane (5 mL) and CNPh (2.2 equiv, 0.2 mL, 1.75 mmol) was added via syringe after stirring at RT for 1 h. The solvent was removed by filtration, and the residue dried in vacuo. The residue was resuspended in hexane (5 mL), GaCp* (3 equiv, 488 mg, 2.38 mmol) was added, and the suspension turned into an orange solution. After a few minutes a red precipitate started to form, and the reaction mixture was reduced in volume to obtain full precipitation. The supernatant solution was filtered off, and the residue dried thoroughly overnight. Yield 230 mg (70%) of an orange powder. Single crystals can be obtained by slow diffusion of hexane into a saturated solution of **4** in toluene. ^{1}H NMR (250.1 MHz, C_6D_6, 24 °C): δ = 7.45 (8H, CN**Ph**), 7.42 (8H, CN**Ph**), 6.99 (4H, CN**Ph**), 2.17 (60H, C_5**Me**$_5$), ppm. $^{13}C\{^1H\}$ NMR (62.9 MHz, C_6D_6, 24 °C): δ = 171.1, 130.0, 129.6, 124.9, 113.3, 10.9 ppm. IR (ATR): 2039 (vs, C≡N), 1976 (shoulder), 1579 (s), 1193 (w, C−N) cm^{-1}. No signals in LIFDI-MS (toluene). Elemental Anal. Calc. for $C_{68}H_{80}Ga_4N_4Pd_4$: C, 49.3; H, 4.9; N: 3.4; found: C: 48.7; H: 5.3; N: 3.2%.

[Ni$_4$GaZn$_7$(Cp*)$_2$Me$_7$(CN*t*-Bu)$_6$] (4). **1** (100 mg, 0.123 mmol) was dissolved together with 2 equiv of GaCp* (50 mg, 0.245 mmol) in toluene (5 mL), a 1.2 M solution of ZnMe$_2$ (14 equiv, 1.4 mL, 1.722 mmol) in toluene was added via syringe, and the mixture was stirred at 100 °C for 2 h, whereby the solution turned into a dark red solution. The reaction mixture was cooled down to RT, and all volatile materials were evaporated in vacuo to obtain a reddish powder in a yield of 131 mg (63%). ^{1}H NMR (250.1 MHz, C_6D_6, 24 °C): δ = 2.51 (15H, C_5**Me**$_5$), 2.36 (15H, C_5**Me**$_5$), 1.35 (60H, CNC**Me**$_3$), 0.15−0.00 (18H, ZnMe). ^{13}C NMR (62.9 MHz, C_6D_6, 24 °C): δ = 110.4, 31.0, 30.5, 11.7 ppm. IR (ATR): 2006 (s, C≡N), 1195 (s, C−N) cm^{-1}. No signals in LIFDI-MS (toluene). Elemental Anal. Calc. for $C_{57}H_{105}Ga_1N_6Ni_4Zn_8$: C: 40.2; H: 6.2; N: 4.9; Zn: 30.7; found: C: 39.7; H: 5.7; N: 4.4; Zn: 30.2%.

[{Pd(CN*t*-Bu)(μ_2-ZnCp*)(μ_3-ZnMe)}$_4$] (5a). **2a** (100 mg, 0.064 mmol) was suspended in toluene (5 mL) at RT, a 1.2 M solution of ZnMe$_2$ (15 equiv, 0.79 mL, 0.95 mmol) in toluene was added via syringe, and the mixture was stirred at RT for 1 h, whereupon the suspension turned into a dark red solution. All volatile materials were evaporated in vacuo to obtain a reddish powder in a yield of 115 mg (96%). ^{1}H NMR (250.1 MHz, C_6D_6, 24 °C): δ = 2.31 (60H, C_5**Me**$_5$), 1.41, (36H, CNC**Me**$_3$) 0.31 (12H, ZnMe) ppm. ^{13}C NMR (62.9 MHz, C_6D_6, 24 °C): δ = 109.6, 30.4, 11.6 ppm. IR (ATR): 2093 (s, C≡N), 2034 (shoulder), 1188 (s, C−N) cm^{-1}. LIFDI-MS (toluene): [M$^+$]: 1881.5 *m*/*z*. Elemental Anal. Calc. for $C_{64}H_{108}N_4Pd_4Zn_8$: C, 40.8; H, 5.8; N: 3.0; Zn: 26.7; found: C: 40.4; H: 5.6; N: 2.9; Zn: 26.3%.

[{Pd(CNPh)(μ_2-ZnCp*)(μ_3-ZnMe)}$_4$] (5b). **4** (100 mg, 0.060 mmol) was dissolved in toluene (5 mL) at RT, a 1.2 M solution of ZnMe$_2$ (15 equiv, 0.75 mL, 0.90 mmol) in toluene was added via syringe, and the mixture was stirred at RT for 1 h, whereupon the suspension turned into to dark red. All volatile materials were evaporated in vacuo to obtain a reddish powder in a yield of 101 mg (85%). ^{1}H NMR (250.1 MHz, C_6D_6, 24 °C): δ = 7.62 (8H, CN**Ph**), 7.46 (4H, CN**Ph**), 6.86 (8H, CN**Ph**), 2.32 (60H, C_5**Me**$_5$), 0.57 (12H, Zn**Me**) ppm. ^{13}C NMR (62.9 MHz, C_6D_6, 24 °C): δ = 130.7, 130.0, 124.8, 110.1, 11.4, 1.43 ppm. IR (ATR): 2045 (s, C≡N), 1968 (shoulder) cm^{-1}. No signals in LIFDI-MS (toluene). Elemental Anal. Calc. for $C_{72}H_{92}N_4Pd_4Zn_8$: C, 44.1; H, 4.7; N: 2.9; found: C, 44.4; H, 4.5; N, 2.6%.

[{Cp*(*t*-Bu)Al($\mu_{1,2}$-CN)}$_4$] (6). [{AlCp*}$_4$] (100 mg, 0.154 mmol) was suspended in toluene (5 mL), excess of CN*t*-Bu (14 equiv, 180 mg, 2.168 mmol) was added via syringe, and the mixture was stirred at 100 °C for 30 min, whereby the suspension turned into a bright yellow almost colorless solution after 10 min. The reaction mixture was cooled down to RT, and all volatile materials were evaporated in vacuo to obtain a colorless powder. Yield 126 mg (84%). ^{1}H NMR (250.1

dx.doi.org/10.1021/ic4022189 | *Inorg. Chem.* 2013, 52, 14275−14283

MHz, C_6D_6, 24 °C): δ = 2.04 (15H, $C_5\mathbf{Me}_5$), 1.00 (9H, CNC$\mathbf{Me}_3$) ppm. ^{13}C NMR (62.9 MHz, C_6D_6, 24 °C): δ = 115.4, 29.8, 29.5, 29.3, 11.9, 11.8, 11.7 ppm. IR (ATR): 2170 (w, C≡N) cm^{-1}. No signals in LIFDI-MS (toluene). Elemental Anal. Calc. for $C_{60}H_{96}N_4Al_4$: C: 73.5; H: 9.86; N: 5.7; found: C: 72.7; H: 10.1; N: 5.2%.

■ ASSOCIATED CONTENT

Supporting Information

Crystallographic data in CIF format. Further details are given in Scheme S1, Figure S1, and Table S1. This material is available free of charge via the Internet at http://pubs.acs.org.

■ AUTHOR INFORMATION

Corresponding Author

*E-mail: roland.fischer@ruhr-uni-bochum.de. Fax: (+49)234 321 4174.

Notes

The authors declare no competing financial interest.

■ ACKNOWLEDGMENTS

The dissertation project of M.M. is supported by the German Chemical Industry Fund (scholarship) and the Ruhr University Research School (http://www.research-school.rub.de). This work was supported by the Deutsche Forschungsgemeinschaft (DFG) Grant Fi-502/23-1/2. We thank the Linden CMS GmbH (http://www.linden-cms.de) and S. Bendix (Ruhr University Bochum) for support in mass spectrometry.

■ REFERENCES

(1) Cadenbach, T.; Gemel, C.; Schmid, R.; Fischer, R. A. *J. Am. Chem. Soc.* **2005**, *127*, 17068−17078.
(2) Bollermann, T.; Gemel, C.; Fischer, R. A. *Coord. Chem. Rev.* **2012**, *256*, 537−555.
(3) Cadenbach, T.; Gemel, C.; Fischer, R. A. *Angew. Chem., Int. Ed.* **2008**, *47*, 9146−9149.
(4) Molon, M.; Cadenbach, T.; Bollermann, T.; Gemel, C.; Fischer, R. A. *Chem. Commun.* **2010**, *46*, 5677−5679.
(5) Bollermann, T.; Schwedler, I.; Molon, M.; Freitag, K.; Gemel, C.; Seidel, R. W.; Fischer, R. A. *Dalton Trans.* **2011**, 12570−12577.
(6) Cadenbach, T. Dissertation Thesis, Ruhr-Universität Bochum, Bochum, Germany, 2009.
(7) Molon, M.; Gemel, C.; Fischer, R. A. *Eur. J. Inorg. Chem.* **2013**, *2013*, 3616−3622.
(8) Molon, M.; Gemel, C.; Seidel, R. W.; Jerabek, P.; Frenking, G.; Fischer, R. A. *Inorg. Chem.* **2013**, *52*, 7152−7160.
(9) Leiner, E.; Scheer, M. *J. Organomet. Chem.* **2002**, *646*, 247−254.
(10) Jutzi, P.; Neumann, B.; Reumann, G.; Stammler, H.-G. *Organometallics* **1998**, *17*, 1305−1314.
(11) Grachova, E. V.; Jutzi, P.; Neumann, B.; Schebaum, L. O.; Stammler, H.-G.; Tunik, S. P. *J. Chem. Soc., Dalton Trans.* **2002**, *0*, 302−304.
(12) Grachova, E. V.; Jutzi, P.; Neumann, B.; Stammler, H.-G. *Dalton Trans.* **2005**, *0*, 3614−3616.
(13) Cokoja, M.; Steinke, T.; Gemel, C.; Welzel, T.; Winter, M.; Merz, K.; Fischer, R. A. *J. Organomet. Chem.* **2003**, *684*, 277−286.
(14) Jutzi, P.; Neumann, B.; Schebaum, L. O.; Stammler, A.; Stammler, H.-G. *Organometallics* **1999**, *18*, 4462−4464.
(15) Bochmann, M.; Hawkins, I.; Yellowlees, L. J.; Hursthouse, M. B.; Short, R. L. *Polyhedron* **1989**, *8*, 1351−1355.
(16) Bennett, M. J.; Cotton, F. A.; Winquist, B. H. C. *J. Am. Chem. Soc.* **1967**, *89*, 5366−5372.
(17) Campbell, G. K.; Hitchcock, P. B.; Lappert, M. F.; Misra, M. C. *J. Organomet. Chem.* **1985**, *289*, c1−c4.
(18) Steinke, T.; Gemel, C.; Winter, M.; Fischer, R. A. *Chem.—Eur. J.* **2005**, *11*, 1636−1646.
(19) Arblaster, J. W. *Platinum Met. Rev.* **1997**, *41*, 12−21.
(20) Arblaster, J. W. *Platinum Met. Rev.* **2012**, *56*, 181−189.
(21) Gemel, C.; Steinke, T.; Weiss, D.; Cokoja, M.; Winter, M.; Fischer, R. A. *Organometallics* **2003**, *22*, 2705−2710.
(22) Cadenbach, T.; Bollermann, T.; Gemel, C.; Tombul, M.; Fernandez, I.; van Hopffgarten, M.; Frenking, G.; Fischer, R. A. *J. Am. Chem. Soc.* **2009**, *131*, 16063−16077.
(23) Edstrom, V. A.; Westman, S. *Acta Chem. Scand.* **1969**, *23*, 279−285.
(24) Bollermann, T.; Molon, M.; Gemel, C.; Freitag, K.; Seidel, R. W.; von Hopffgarten, M.; Jerabek, P.; Frenking, G.; Fischer, R. A. *Chem.—Eur. J.* **2012**, *18*, 4909−4915.
(25) Jutzi, P.; Schebaum, L. O. *J. Organomet. Chem.* **2002**, *654*, 176−179.
(26) Schormann, M.; Klimek, K. S.; Hatop, H.; Varkey, S. P.; Roesky, H. W.; Lehmann, C.; Roepken, C.; Herbst-Irmer, R.; Noltemeyer, M. *J. Solid State Chem.* **2001**, *162*, 225−236.
(27) Schulz, S.; Roesky, H. W.; Koch, H. J.; Sheldrick, G. M.; Stalke, D.; Kuhn, A. *Angew. Chem.* **1993**, *105*, 1828−1830; *Angew. Chem., Int. Ed. Engl.* **1993**, *1832* (1812), 1729−1831.
(28) Thomas, M. G.; Pretzer, W. R.; Beier, B. F.; Hirsekorn, F. J.; Muetterties, E. L. *J. Am. Chem. Soc.* **1977**, *99*, 743−748.
(29) Day, V. W.; Day, R. O.; Kristoff, J. S.; Hirsekorn, F. J.; Muetterties, E. L. *J. Am. Chem. Soc.* **1975**, *97*, 2571−2573.
(30) Fischer, E. O.; Werner, H. *Chem. Ber.* **1962**, *95*, 703−708.
(31) De Graaf, W.; Boersma, J.; Smeets, W. J. J.; Spek, A. L.; Van Koten, G. *Organometallics* **1989**, *8*, 2907−2917.
(32) Green, M.; Howard, J. A. K.; Murray, M.; Spencer, J. L.; Stone, F. G. A. *J. Chem. Soc., Dalton Trans.* **1977**, 1509−1514.
(33) Green, M.; Howard, J. A. K.; Spencer, J. L.; Stone, F. G. A. *J. Chem. Soc., Chem. Commun.* **1975**, 449−451.
(34) Spencer, J. L. *Inorg. Synth.* **1979**, *19*, 213−218.
(35) Hübschle, C. B.; Sheldrick, G. M.; Dittrich, B. *J. Appl. Crystallogr.* **2011**, *44*, 1281−1284.
(36) Sheldrick, G. M. *SHELXL-97, Program for refinement of crystal structures*; University of Göttingen: Göttingen, Germany, 1997.
(37) Van Der Sluis, P.; Spek, A. L. *Acta Crystallogr., Sect. A* **1990**, *46*, 194−201.
(38) Spek, A. L. *J. Appl. Crystallogr.* **2003**, *36*, 7−13.